Forecast Techniques

A METHOD FOR DIAGNOSING VERTICAL MOTION
AND SURFACE PRESSURE TENDENCY FROM
LFM ANALYSES

by

Toby N. Carlson (1)
Associate Professor

Department of Meteorology
The Pennsylvania State University
University Park, PA 16802

1. INTRODUCTION

Vertical motion and sea-level pressure tendency are important atmospheric variables, the former being related to the distribution of cloudiness and precipitation and the latter to the development and movement of weather systems. Although the sense of the vertical motion may be apparent from the weather itself and the isallobaric pattern can be analyzed routinely from the reported sea-level pressure tendencies, it is not particularly useful to diagnose either of these fields without consideration of large-scale upper air flow which can provide the insight into the evolution of weather patterns. It is customary for weather forecasters to examine the 500 mb height and vorticity charts and the 1000-500 mb thickness fields, products which are customarily provided by the National Weather Service, and to equate upward (or downward) vertical motion and falling (or rising) sea-level pressures with regions of positive (or negative) absolute 500 mb vorticity advection and with warm (or cold) thickness advection.

This association between upper air patterns and surface cyclone behavior is discussed by Petterssen (2). A lucid account of the relationship between vertical motion and surface pressure tendency and the configuration of highs, and lows, troughs and ridges is presented by Holton (3). With the aid of simplifying assumptions, Holton reduced the differential form of the omega and pressure tendency equations to simple algebraic expressions relating the geostrophic vorticity advection and thickness advection to the vertical motions (or sea-level pressure tendency). The geostrophic advection terms in these equations are sometimes referred to as "forcing functions", although this description is misleading since the atmosphere is not being forced by its internal dynamics. Nevertheless, the concept of

forcing is extremely useful since it allows one to diagnose the vertical motions and the surface pressure changes in terms of geostrophic advections, which are easy to evaluate using conventional weather charts of geopotential height, vorticity and thickness. Since numerical weather prediction models do not usually produce useful initial vertical motion information, this technique may serve as another approach.

In this paper we will describe briefly a simple one-layer quasi-geostrophic model in Section 2 and use the derived relationships in the model in Section 3 to illustrate a method for diagnosing the lower-tropospheric vertical motion and sea-level pressure tendency associated with the geostrophic advection of vorticity and temperature. Nomograms are provided for evaluating the vertical motion and surface pressure tendency from conventional LFM height, vorticity and thickness analyses.

2. THE METHOD

Let us consider the form of the quasi-geostrophic omega equation

$$\frac{R_d}{gp} \tilde{s} \nabla^2 \omega + \frac{\tilde{f}^2}{g} \frac{\partial^2 \omega}{\partial p^2} =$$

$$-\frac{f}{g} \frac{\partial}{\partial p} [-\vec{V} \cdot \nabla(\zeta + f)] + \nabla^2 (-\vec{V} \cdot \nabla \frac{\partial z}{\partial p}) \qquad (1)$$

where $\vec{V}$ is the geostrophic advecting velocity, z the geopotential height, p the pressure, $\tilde{f}$ the Coriolis parameter (locally a constant), $\tilde{s}$ a static stability (also locally a constant and equal approximately to the change in potential temperature with pressure, $-\partial\theta/\partial p$), R_d the gas constant for dry air, g the gravitational constant, ζ the relative geostrophic vorticity and ω $(=dp/dt)$ is the vertical motion.

Our solution to this equation follows Holton (3) and is based on the following assumptions: (a) the vertical wind shear is constant with height between 1000 and 500 mb; (b) all height, temperature and vorticity patterns vary sinusoidally in x and y; varies sinusoidally in x, y and p; (c) all vertical derivatives are taken as finite differences between 1000 and 500 mb. With these assumptions Equation (1) reduces to an equation of the form

$$- \omega_7 \simeq -\bar{\omega}^p =$$

$$A \left[-\vec{\mathcal{V}}_5 \cdot \nabla Q_5 + \vec{\mathcal{V}}_0 \cdot \nabla Q_0 \right] + B \left(-\mathcal{V}_0 \cdot \nabla h \right) \qquad (2)$$

where h is the 1000 to 500 mb thickness, Q is the absolute vorticity ($= \zeta + f$), and the subscripts 0, 7, and 5 refer to the 1000, 700, 500 mb levels respectively. ω^{-p} is considered to be representative vertical motion over the 1000 and 500 mb layer, which we assume is centered approximately at 700 mb. Equation (2) thus represents an averaged omega equation over the 1000 to 500 mb layer. The terms A and B are defined as follows,

$$A = \frac{\Delta p_o^2}{\Delta p_5 f \pi^2 (1 + L_R^2 / L^2)} \qquad (3a)$$

$$B = \frac{8g \Delta p_o^2}{L^2 \Delta p_5 \tilde{f}^2 (1 + L_R^2 / L^2)} \qquad (3b)$$

where Δp_o is the depth of the disturbance (normally 900 mb), $\Delta p_5 = 500$ mb, L is the wavelength of the disturbance and

$$L_R \equiv \left[\frac{8R_d}{\bar{p}} \left(\frac{\tilde{s} \Delta p_o^2}{\tilde{f}^2} \right) \right]^{1/2}$$

where $\bar{p} \equiv 700$ mb. Details of the derivation of these relationships and of the model in general an be found in Carlson (4).

The quasi-geostrophic vorticity equation (2) can be written as

$$\partial \zeta / \partial t = A_Q - QD \qquad (4)$$

where A_Q is the advection of absolute vorticity $\tilde{} (-\vec{V} \cdot \nabla(\zeta + f))$ and D is the horizontal divergence $(= \partial u / \partial x + \partial v / \partial y)$. Thus, when the divergence is positive (negative)

there will be a local spin down (spin up) of the relative vorticity which, in a geostrophically balanced atmosphere, implies local pressure rises (falls). Realizing the D = $-\partial \omega / \partial p$, in the absence of a strong terrain influence, the vertical motion at the surface is generally much smaller at the surface than that at 700 mb in active weather situations at middle latitudes. Consequently, rising (sinking) motion at 700 mb corresponds to low-level convergence (divergence) and pressure falls (rises) at the surface. Accordingly, one can use the results of the omega equation (2) to diagnose the sea-level pressure tendencies.

Settings $D_O = \frac{\omega_7}{300 \text{ mb}}$, ignoring the surface vorticity advection (which will be small in most cases compared to the divergence term in Equation (4)) and inserting Equation (2) into (4) with the assumption of sinusoidal variation of vorticity leads to the equation

$$\frac{\partial p_s}{\partial t} = - \{ A'(-\vec{V}_5 \cdot \nabla Q_5) + B'(-\vec{V}_0 \cdot \nabla h) \} \qquad (5)$$

where $\frac{\partial p_s}{\partial t}$ is the sea-level pressure tendency and A' and B' are analogous to A and B in Equation (3) except that

$$A' = \frac{\tilde{f} L^2 \Delta p_o^2}{8 \pi^4 g \Delta p_5 \Delta p_3 K (1 + L_R^2 / L^2)} \qquad (6a)$$

$$B' = \frac{\Delta p_o^2}{\pi^2 \Delta p_5 \Delta p_3 K (1 + L_R^2 / L^2)} \qquad (6b)$$

where $\Delta p_3 \equiv 300$ mb and K is a conversion between changes in pressure at sea level (subscript s) and changes in height at the corresponding 1000 mb surface; it is approximately 8 m (mb)$^{-1}$.

Equations (2) and (5) express the vertical motions and sea-level pressure tendency as linear sums of vorticity and thickness advections. It is possible to evaluate these advections by inspection of conventional analyses provided by the National Weather Service on the LFM facsimile charts as follows: The advection of a quantity q by the geostrophic wind is

$$A_q = g / \tilde{f} \frac{\Delta z}{\Delta n} \frac{\Delta q}{\Delta s} = C / S_q \qquad (7)$$

where Δn and Δs are distances taken, res-

pectively, normal to and along the geostrophic wind vector. In Equation (7) C ($= g/\bar{f} \, \Delta z \Delta q$) is a constant defined by the contour intervals of height and q which are, respectively, Δz and Δq. S_q is the solenoidal area formed by the intersection of adjacent pairs of height and q isopleths. A discussion of the solenoid concept for evaluating geostrophic advection is given by Petterssen (2). In the case of 500 mb absolute vorticity advection the 500 mb height contour interval (Δz_5) is 60 m and the interval between vorticity isopleths (ΔQ_5) is $2 \times 10^{-5} s^{-1}$ on the LFM charts. S_Q is the horizontal area of the solenoids formed by height and vorticity contours. For the thickness advection it is convenient to approximate the 4 mb intervals of sea-level pressure on the LFM sea-level pressure chart as 30 m intervals on an equivalent 1000 mb height surface. Thus, for thickness advection, the height contour interval (Δz_0) is 30 m and the thickness contour interval (Δh) is 60 m. S_h is the area of the solenoid formed by height and thickness contours.

Examples of both 500 mb vorticity advection and thickness advection solenoids (S_Q and S_h) on the LFM initial analyses are shown by the shaded areas in Figures 1 and 2. The solenoid depicted by the shaded area in each figure represents one of a number of positive and negative advection solenoids associated with the wave cyclone over southern Canada. The

shaded vorticity and thickness solenoids in each figure are approximately co-located and represent positive advection. Of course, significant positive advection can exist without the appearance of solenoids because the contour intervals used in the LFM analyses may be too large to allow a complete four-sided figure to be formed even when the crossing angle between geostrophic wind and isopleths of Q or h is large. In such instances the geostrophic advections can be determined by constructing additional intermediate height and vorticity (or thickness) isopleths.

In Figures 1 and 2, the heavy shaded square over the Atlantic Ocean, labelled unit solenoid, corresponds to a <u>unit</u> area of a 1° x 1° latitude (110 x 110 $\overline{\text{km}}$) solenoid. It is convenient in evaluating the area of a solenoid to refer to a solenoid <u>number</u> representing the ratio of the actual solenoidal area to that of a unit solenoid, whose value of advection is known. For convenience we have evaluated all coefficients in Equations (2) through (6) for a unit advection solenoid. Therefore, Equations (2) and (5) are rewritten

$$- \omega_7 = c_1/n_1 + c_2/n_2 \qquad (8a)$$

$$- \frac{\partial p_s}{\partial t} = c_1'/n_1 + c_2'/n_2 \qquad (8b)$$

where n_1 and n_2, respectively, are the solenoid numbers (the ratio of observed solenoidal area to the unit solenoidal area) for the 500 mb vorticity advections
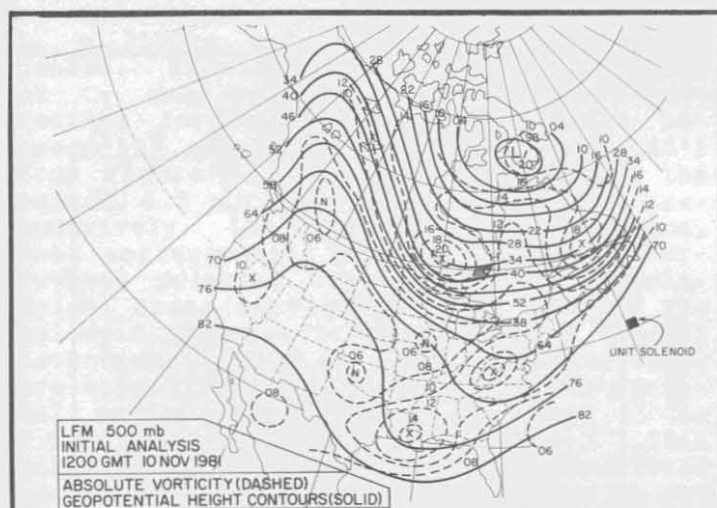

Figure 1. LFM initial analyses of the 500 mb geopotential height contours (solid lines labelled in dm above 500) and absolute vorticity isopleths (dashed lines labelled in $10^{-5} s^{-1}$) for 1200 GMT, 10 November 1981. The shaded area east of the surface low over southern Canada corresponds to a positive advection solenoid. The arrowhead pointing to the open circle adjacent to the solenoid is the location of the calculation referred to in the text.
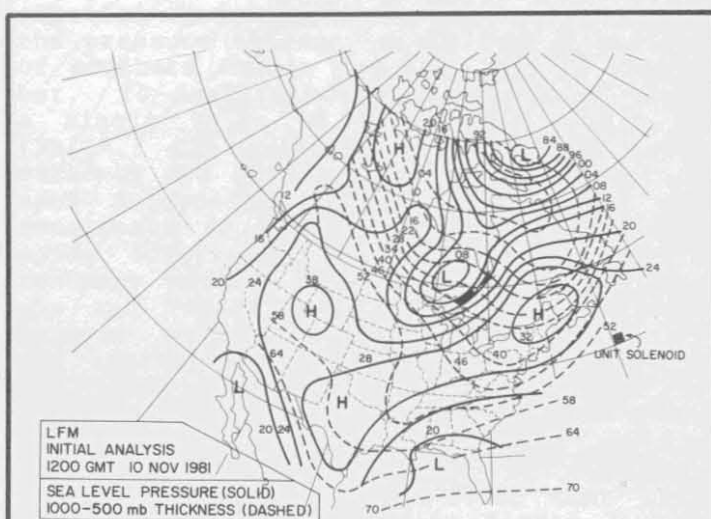

Figure 2. LFM initial analyses of the sea-level pressure (solid lines labelled in mb above 1000) and 1000-500 mb thickness contours (dashed lines labelled in dm above 500) for 1200 GMT, 10 November 1981.

and the 1000-500 mb thickness advections; C_1 C_2, C_1' and C_2' are pseudo constants (the analogs of A, B, A' and B'; in Equations (2) and (5)), which depend principally on wavelength, stability and latitude. For given values of the constants the vertical motion and sea-level pressure tendency equal sums of weighted inverse solenoid numbers for vorticity and thermal advections.

3.   APPLICATION OF THE MODEL

Inspection of Figures 1 and 2 reveals strong advection patterns for both vorticity and thickness. Pressure falls and rises of about 4 mb per 3h were observed, respectively east and west of the surface low, which had been moving eastward across southern Canada (Figure 3). Relatively small advection solenoids in Figures 1 and 2 correspond to areas of strongest pressure tendency in Figure 3.

By inspection it is found the shaded vorticity advection solenoid in Figure 1 contains about 3.5 unit solenoids. The thermal advection solenoid shaded in Figure 2 contains about 2.0 unit solenoids. In order to translate these solenoid numbers into values of vertical motion and sea-level pressure tendency, it is necessary to consult the coefficient nomograms for the unit advection solenoids (Figures 4-7), which were determined for a latitude of 40° and a disturbance depth (Δp_0) of 900 mb. For a particular value of stability ($\tilde{s}$), latitude and atmospheric depth,

L_R is fixed. For fixed values of Δp_0 and latitude, the variation between L_R and $\tilde{s}$ is shown in Figure 8. At a given latitude L_R is governed primarily by variations in static stability if the depth of the disturbance is a large fraction of 1000 mb. Although one could measure the large scale value of the 1000 to
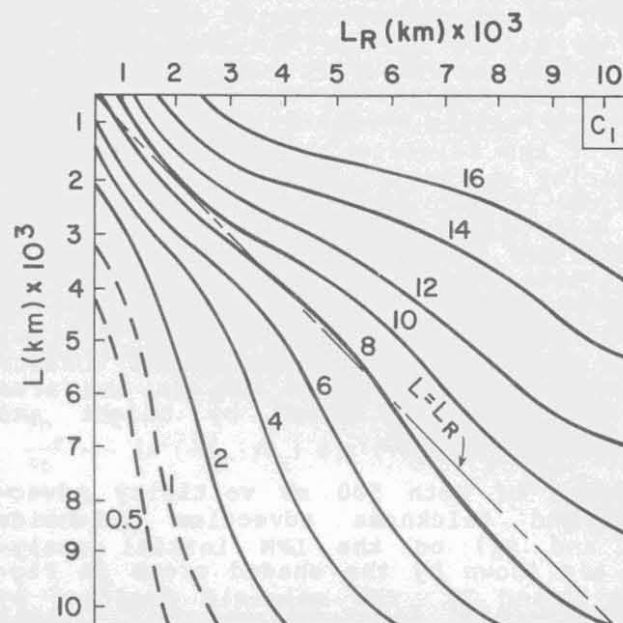

Figure 4. Nomogram of the vorticity advection coefficient (C_1; units b s^{-1}) for the vertical motion ($-\omega$) at 40° latitude.

Figure 3. Observed 3 hr sea-level pressure tendency 1900-1200 GMT, 10 November 1981 (solid lines labelled in mb (3h)$^{-1}$; surface fronts added). The arrowhead east of the surface low has the same meaning as in Figures 1 and 2.
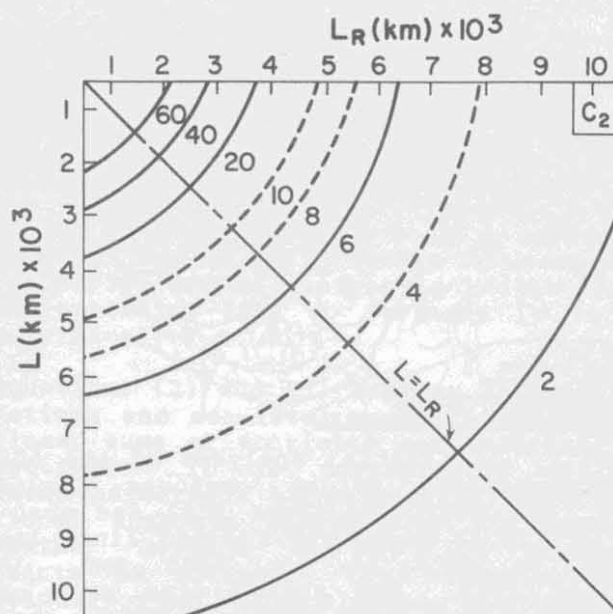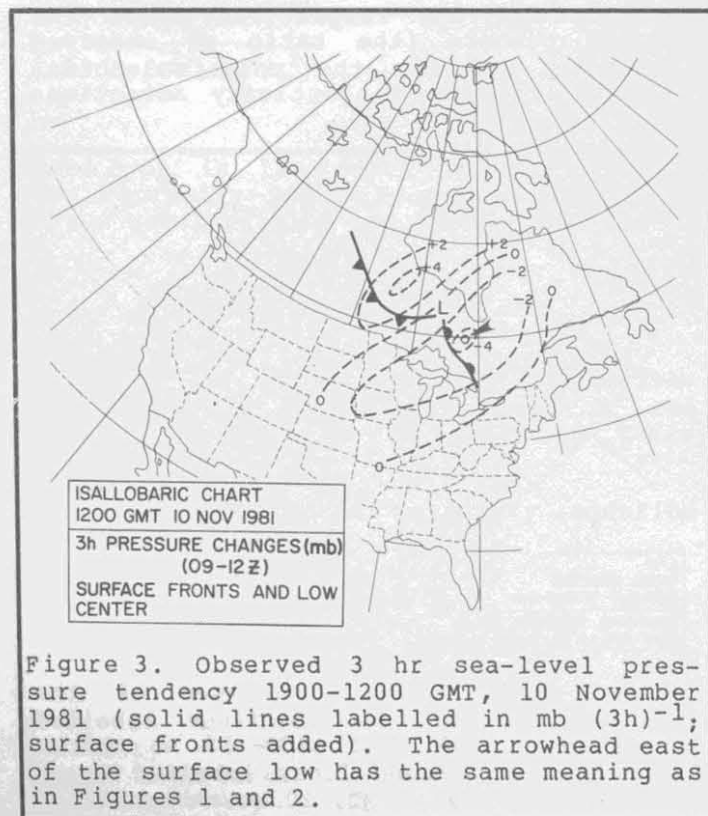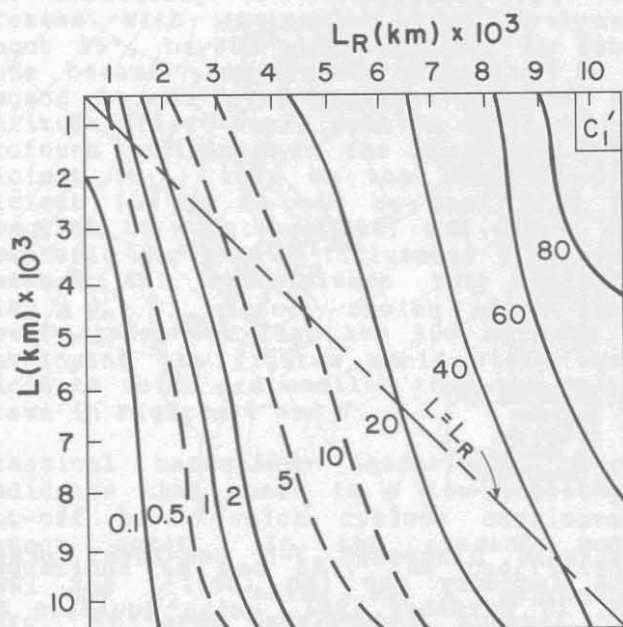

Figure 5. Nomogram for the thickness advection coefficient C_1' (units mb(3h)$^{-1}$) for the sea-level pressure tendency at 40° latitude.

Figure 6. Nomogram of the vorticity advection coefficient C_1' (units mb $(3h)^{-1}$) for the sea-level pressure tendency   at 40° latitude.
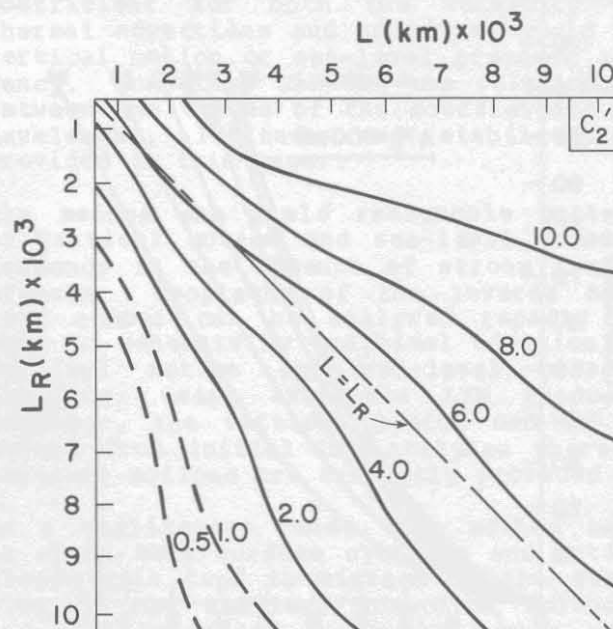

Figure 7. Nomogram of the thickness advection coefficient C_2' (units mb$(3h)^{-1}$) for the sea-level pressure tendency   at 40° latitude.

500 mb static stability (5), an expedient choice of the characteristic length scale (L_R) is that of the measured wavelength which is typically about 3500 km.

As an example, let us suppose that $L = L_R = 3500$ km for the wave over southern Canada. From Figures 4 and 5 the values of C_1 and C_2 are obtained after correcting for the latitude difference between 50° and the reference latitude (40°) from Figure 9. These constants have the values 6.3 μb s^{-1} and 7.2 μb s^{-1}, respectively. Let us consider one location, that corresponding to the tip of the arrowhead pointing toward the shaded solenoidal areas of Figures 1 and 2 where the solenoid numbers for vorticity and thermal advections (n_1 and n_2, respectively) are approximately 3.5 and 2.0. The vertical motion $(-\omega_7)$ there is found to be 5.5 μb s^{-1} from Equation (8a). This value somewhat exceeds the LFM predicted ascent of 2.0 μb s^{-1} for 1200 GMT 10 November 1981.

Similarly, at this same location, C_1' and C_2' are found to be 5.7 mb $(3h)^{-1}$ and 4.7 mb $(3h)^{-1}$, respectively, from Figures 6 and 7 when corrected to 50° latitude using the values provided in Figure 9. At the location of the arrowhead in Figures 1 and 2, the sea-level pressure tendency from Equation (8b) is found to be 3.7 mb $(3h^{-1})$, which is close to the reported value of 4 mb $(3h^{-1})$ at the corresponding location in Figure 3.

It has been our experience that this approach for determining patterns of vertical motion and sea-level pressure tendency is satisfactory in the absence of strong terrain effects, although the derived quantities are likely to be underestimated in regions of large-scale condensation.

To further illustrate the ability of the model for determining reasonable and useful patterns with relatively little effort expended at computation, we have analyzed the pressure tendency field over a portion of southern Canada for 1200 GMT 10 November. To facilitate the analyses we chose a single value of $C_1' = C_2' = 5.0$ mb $(3h)^{-1}$. The solenoid numbers were estimated by eye and recorded at the center of each solenoid. The solenoid number was considered to be infinity where no solenoids occurred. The sea-level pressure tendency pattern was determined by a simple and rapid graphical addition of the inverse solenoids numbers for vorticity and thermal advections. The sum of the two terms in Equation (8b) yielded the sea-level pressure tendency pattern shown in Figure 10. The isallobaric maximum west of the surface low in Figure 10 was located somewhat farther south than that of the observed maximum in Figure 3, but the overall shape and strength of the derived pressure change pattern closely resembles those of the observed pattern. Our experience has shown that choosing approximate values of about 5.0 mb $(3h)^{-1}$ for the constants C_1' and C_2' and 4.0
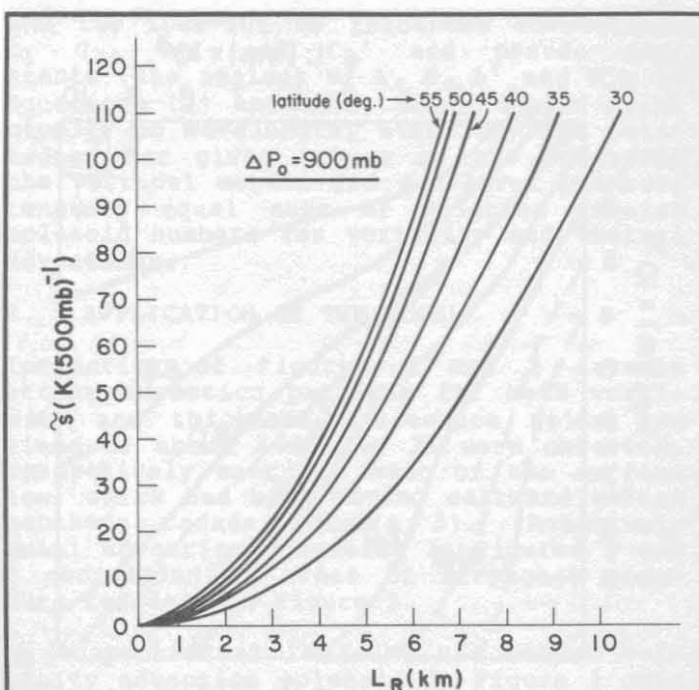
Figure 8. Relationship between L_R and the stability s for different latitudes.
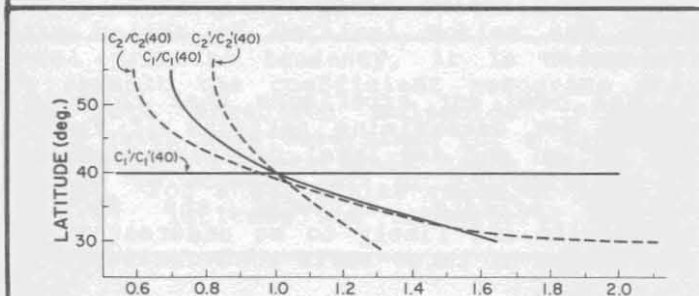

Figure 9. Latitude correction factor for the coefficients in Figures 4-7. The correct value of the coefficient can be obtained by multiplying the numbers in this figure by the value of the coefficients at 40° obtained from Figures 4-7.

$\mu b\ s^{-1}$ for C_1 and C_2 yields reasonable patterns of sea-level pressure tendency and vertical motion in a variety of situations where terrain influences are negligible. It is perhaps fortuitous that the coefficients C_1 and C_2 (or C_1' and C_2') are generally about equal since this implies vorticity advection and thermal advection solenoids contribute approximately identical forcing to the sea-level pressure tendency or vertical motion. Thermal advections, however, appear to be broader and less sharply focused than vorticity advections.

4. THEORETICAL CONSIDERATIONS

The values of the coefficients in Figures 4 through 7 represent a measure of the ef-
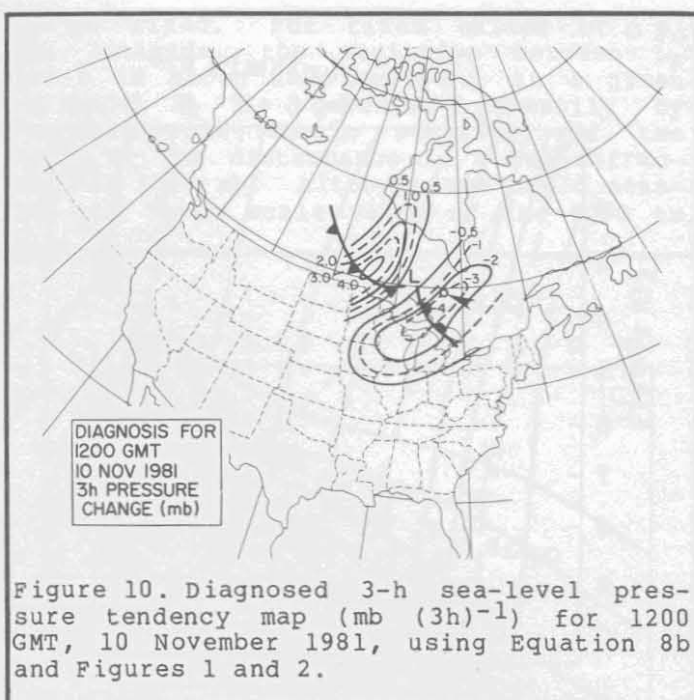

Figure 10. Diagnosed 3-h sea-level pressure tendency map (mb $(3h)^{-1}$) for 1200 GMT, 10 November 1981, using Equation 8b and Figures 1 and 2.

ficiency with which the vorticity or thermal advections are translated into vertical motions or sea-level pressure tendency. For a given advection solenoid, the long waves are generally more efficient in forcing the sea-level pressure tendency (Figures 6 and 7) although the situation is ambiguous with regard to the vertical motions because of the opposite variation in C_1 and C_2 with respect to L.

The forcing is more efficient for lower stability (smaller L_R) which is to say that when a cyclone encounters a region of diminished static stability, the propensity for it to develop becomes enhanced. Examples of cyclone intensification in the presence of reduced static stability abound in the literature. With reduced static stability, however, the preferred growth rate of disturbances occurs at shorter wavelengths so that a disturbance encountering a region of lower static stability might begin to form a shorter wave within a longer one. In a relatively stable atmosphere the short waves are quite inefficient in producing sea-level pressure changes, as can be seen in Figures 6 and 7.

Classical baroclinic instability theory suggests that the most efficient wavelength for cyclone growth is close to L_R, which diminishes in magnitude with decreasing stability for a given latitude and disturbance depth (Figure 8). For large values of L_R (large stability) and small wavelengths the thickness advection term becomes relatively insignificant, whereas for small values of L_R and L, the thickness advection dominates.

The efficiency of the forcing also increases with increasing latitude until about 55°, beyond which changes in latitude become unimportant (Figure 9). In regard to sea-level pressure changes, the latitude effect would seem to exert a more profound influence in the vorticity coefficient (C_1') than on the thermal coefficient (C_2'), as can be seen from inspection of Equations (6a) and (6b). Atmospheric depth also influences efficiency because all coefficients vary directly with $\Delta p_0{}^2$. Hence, choice of a shallower atmosphere than the 900 mb used in developing the figures would yield coefficients which are smaller than the values drawn in Figures 6 and 7.

Classical baroclinic instability theory indicates that there is a low wavelength cut-off below which cyclone development cannot occur. In the present model (Equations 6a and 6b), the coefficients C_1' and C_2' vanish as L approaches zero. At large wavelengths, however, the coefficients for sea-level pressure tendency (Figures 6 and 7) increase boundlessly although C_2' approaches a constant value at large L. However, long wavelengths tend to be associated with small advection, partly because the centers of maximum and minimum vorticities or thicknesses are separated by large distances.

5.   SUMMARY AND CONCLUSIONS

A method is presented whereby the 700 mb vertical motions and sea-level pressure tendencies can be diagnosed from inspection of analyses of 500 mb height and absolute vorticity and the sea-level isobars and 1000-500 mb thicknesses. The method for translating patterns of advections from the analyses to vertical motions and sea-level pressure changes is based on a highly simplified solution of the omega and vorticity equations. Both the vertical motion, and sea-level pressure tendencies are determined as the algebraic sum of two geostrophic advections, the 500 mb absolute vorticity advection and the 1000-500 mb thickness advection, each of which is multiplied by coefficients which are dependent primarily on wavelength, static stability and latitude.

The geostrophic advections can be assessed quantitatively by comparing the areas of advection solenoids, formed by the intersection of adjacent height and vorticity (or thickness) contours, with a unit advection solenoid. The inverse solenoid number, which is the ratio of the unit solenoid area to the observed solenoidal area, is multiplied by its appropriate coefficient for both the vorticity and thermal advections and summed to yield the vertical motion or sea-level pressure tendency. Nomograms showing the relationship between the values of the coefficients and wavelength, latitude and stability are provided in this paper.

The method can yield reasonable patterns of vertical motion and sea-level pressure tendency in the absence of strong terrain effects. Isopleths of the inverse solenoid number can be analyzed rapidly and used to generate by graphical addition the vertical motion and sea-level pressure tendency, using available LFM products. Moreover, the vertical motion can be assessed from initial LFM analyses where no vertical motions are currently provided.

In a qualitative sense, the method makes it clear that surface cyclones and anticyclones will tend to migrate in the direction of the smallest advection solenoids and will intensify (or weaken) when positive (negative) solenoids exist over the center of the low or high or where there is a predominance of positive (negative) advection solenoids over the feature as a whole. The intensity of the derived patterns will be greater in regions of low static stability such as over warm ocean, currents, over the Great Plains in spring or early summer, and in regions experiencing large-scale moist ascent. Cyclone development will also be more rapid at higher latitudes.

REFERENCES AND FOOTNOTES

1.   Toby N. Carlson earned his B.S. and M.S. degrees at MIT in Boston, MA and his Ph.D. at the University of London. He joined the Meteorology Department at Pennsylvania State University in 1974. He has been active in numerous studies, including tropical research and GATE projects. His current interests involve terrain modeling and soil moisture studies.

2.   Petterssen, S., 1956: Weather Analysis and Forecasting, Vol. 2, Motion and Motion Systems, 2nd Ed., McGraw-Hill, New York, 428 pp.

3.   Holton, J. R., 1972: An Introduction to Dynamic Meteorology, Academic Press, New York, 319 pp.

4.   Carlson, T.N. 1982: A simple model illustrating baroclinic development. Bull. Amer. Meteor. Soc., 63, 1302-1308.

5.   Determined by subtraction of the surface potential temperature from that at 500 mb and dividing by 500 mb.